The spectrum of kidney biopsies in hospitalized patients with COVID-19, acute kidney injury, and/or proteinuria

Sophie Ferlicot[1,2,3]*, Matthieu Jamme[4,5]*, François Gaillard[6]*, Julie Oniszczuk[7]*, Aymeric Couturier[5,8], Olivia May[9], Anne Grünenwald[10,11,12], Aurélie Sannier[3,13], Anissa Moktefi[3,14], Ophélie Le Monnier[15], Camille Petit-Hoang[16], Nadine Maroun[17], Albane Brodin-Sartorius[18], Arthur Michon[11], Hélène Dobosziewicz[11], Fabrizio Andreelli[19], Matthieu Guillet[11], Hassane Izzedine[20], Christian Richard[10], Manon Dekeyser[11], Romain Arrestier[21], Thomas Sthelé[7], Edouard Lefèvre[11], Alexis Mathian[15], Christophe Legendre[11], Charlotte Mussini[1,3], Marie-Christine Verpont[22], Nicolas Pallet[23], Zahir Amoura[15], Marie Essig[5,8], Renaud Snanoudj[18], Isabelle Brocheriou-Spelle[3,24], Hélène François[16], Xavier Belenfant[9], Guillaume Geri[5,25], Eric Daugas[6], Vincent Audard[7], David Buob[3,26], Ziad A. Massy[5,8], Mohamad Zaidan[2,11,27] on behalf of the AP-HP / Universities / Inserm COVID-19 research collaboration.

* These authors contributed equally and share first authorship

1 Service d'Anatomie Pathologique, Assistance Publique-Hôpitaux de Paris (APHP) Université Paris Saclay, Hôpital Bicêtre, Le Kremlin-Bicêtre, France

2 Université Paris Saclay, Université Paris-Sud, UVSQ, Villejuif, France

3 Club Francophone de Pathologie Rénale (CFPR) group

4 Service de Réanimation polyvalente, CH Intercommunal de Poissy Saint Germain en Laye, Poissy, France

5 INSERM U1018, Equipe 5, CESP (Centre de Recherche en Épidémiologie et Santé des Populations), Université Paris Saclay et Université Versailles Saint Quentin en Yvelines), Villejuif, France

6 Service de Néphrologie, Hôpital Bichat, Assistance Publique-Hôpitaux de Paris (APHP), Université de Paris, INSERM U1149, Paris, France

7 Service de Néphrologie et Transplantation, Centre de Référence Maladies Rares « Syndrome Néphrotique Idiopathique », Assistance Publique-Hôpitaux de Paris (APHP), Hôpitaux Universitaires Henri-Mondor, Univ Paris Est Créteil, Institut National de la Santé et de la Recherche Médicale (INSERM) U955, Créteil, France

8 Service de Néphrologie et Dialyse, Assistance Publique-Hôpitaux de Paris (APHP), Hôpital Universitaire Ambroise Paré, Boulogne Billancourt, France

9 Service de néphrologie-dialyse, GHT Grand Paris Nord Est, Hôpital André Grégoire, Montreuil sous Bois

10 Service de médecine intensive-réanimation, Assistance Publique-Hôpitaux de Paris (APHP), Hôpital Bicêtre, Assistance Publique-Hôpitaux de Paris (APHP), 94270 Le Kremlin-Bicêtre, France

11 Service de Néphrologie, Dialyse et Transplantation, Hôpital Bicêtre, Assistance Publique-Hôpitaux de Paris (APHP), 94270 Le Kremlin-Bicêtre, France

12 Centre de Recherche des Cordeliers, INSERM, Sorbonne Université, Université de Paris, Paris, France

13 Université de Paris, Assistance Publique-Hôpitaux de Paris (APHP), Service d'Anatomie et Cytologie Pathologiques, Hôpital Bichat, F-75018, Paris, France

14 Service d'Anatomie Pathologique, Assistance Publique-Hôpitaux de Paris (APHP), Hôpitaux Universitaires Henri-Mondor, Univ Paris Est Créteil, Institut National de la Santé et de la Recherche Médicale (INSERM) U955, Créteil, France

15 Sorbonne Université, Assistance Publique–Hôpitaux de Paris, Groupement Hospitalier Pitié–Salpêtrière, French National Referral Center for Systemic Lupus Erythematosus, Antiphospholipid Antibody Syndrome and Other Autoimmune Disorders, Service de Médecine Interne 2, Institut E3M, Inserm UMRS, Centre d'Immunologie et des Maladies Infectieuses (CIMI-Paris), Paris, France

16 Service UNTR, Assistance Publique-Hôpitaux de Paris (APHP), INSERM 1155, Sorbonne Université, Hôpital Tenon, Paris, France

17 Service de Néphrologie et Dialyse, CH Intercommunal de Poissy Saint-Germain-en-Laye, Poissy, France

18 Service de Néphrologie-Dialyse-Transplantation, Hôpital Foch, Suresnes, France

19 Service de Diabétologie-Métabolismes, Assistance Publique-Hôpitaux de Paris (APHP), CHU Pitié-Salpêtrière, Sorbonne Université, Paris, France

20 Service de Néphrologie, Hôpital Privé des Peupliers, Ramsay Générale de Santé, Paris, France

21 Service de Médecine Intensive Réanimation, Hôpitaux Universitaires Henri-Mondor, Assistance Publique-Hôpitaux de Paris (APHP), Univ Paris Est Créteil, Créteil, France

22 Sorbonne Université, Université Pierre et Marie Curie Paris 06, and Institut National de la Santé et de la Recherche Médicale, Unité Mixte de Recherche S1155, plate-forme d'Imagerie et de Cytométrie de Tenon, F-75020, Paris, France

23 Service de Biochimie, Assistance Publique-Hôpitaux de Paris (APHP), Hôpital Européen Georges Pompidou, Paris, France

24 Sorbonne Universités, UPMC Univ Paris 06, UMR_S 1155, Assistance Publique-Hôpitaux de Paris, Pathology department, Hôpital de la Pitié-Salpêtrière

25 Service de Médecine Intensive Réanimation, Assistance Publique-Hôpitaux de Paris (APHP), Hôpital Universitaire Ambroise Paré, Boulogne Billancourt, France

26 Sorbonne Université, Assistance Publique-Hôpitaux de Paris (APHP), Service d'Anatomie et Cytologie Pathologiques, Hôpital Tenon, F-75020, Paris, France

27 INSERM U1163, Institut IMAGINE, Hôpital Necker-Enfants malades, 75005 Paris, France

Correspondence to: Mohamad Zaidan; E-mail: mohamad.zaidan@aphp.fr

Short title: COVID-19-associated nephropathy

ABSTRACT

We report a multicentric retrospective case series of patients with COVID-19 who developed acute kidney injury and/or proteinuria and underwent a kidney biopsy in the Paris and its metropolitan area.

Forty-seven patients (80.9% men) with COVID-19 who underwent a kidney biopsy between March 08 and May 19, 2020 were included. Median age was 63 years IQR [52-69]. Comorbidities included hypertension (66.0%), diabetes mellitus (27.7%), obesity (27.7%), history of chronic kidney (25.5%), cardiac (38.6%) and respiratory (27.3%) diseases. Initial symptoms were fever (85.1%), cough (63.8%), shortness of breath (55.3%), and diarrhea (23.4%). Almost all patients developed acute kidney injury (97.9%) and 63.8% required renal replacement therapy. Kidney biopsy showed two main histopathological patterns, including

acute tubular injury in 20 (42.6%) patients, and glomerular injury consisting of collapsing glomerulopathy and focal segmental glomerulosclerosis in 17 (36.2%) patients.

Two (4.3%) patients had acute vascular nephropathy, while eight (17%) had alternative diagnosis most likely unrelated to COVID-19. Acute tubular injury occurred almost invariably in the setting of severe forms of COVID-19, whereas patients with glomerular injury had various profiles of COVID-19 severity and collapsing glomerulopathy was only observed in patients harboring a combination of *APOL1* risk variants. At last follow-up, 16 of the 30 patients who initially required dialysis were still on dialysis, and 9 died.

The present study describes the spectrum of kidney lesions in patients with COVID-19. While acute tubular injury is correlated with COVID-19 severity, the pattern of glomerular injury is intimately associated with the expression of *APOL1* risk variants.

Keywords: acute tubular injury, collapsing glomerulopathy, COVID-19, focal segmental glomerulosclerosis, kidney

KEY LEARNING POINTS

What is already known about this subject?

COVID-19 is burdened by a high frequency of kidney injury, proteinuria, and hematuria, which may have a dramatic impact on patients' survival.

What this study adds?

COVID-19-associated nephropathy includes predominant tubular damage in most severe respiratory cases, and collapsing glomerulopathy and focal segmental glomerulosclerosis in non-critically ill patients. The occurrence of collapsing glomerulopathy is highly correlated with the expression of high-risk *APOL1* genotypes.

What impact this may have on practice or policy?

Kidney biopsy and *APOL1* genotyping are necessary to characterize acute kidney involvement during COVID-19.

INTRODUCTION

In December 2019, a novel coronavirus disease 2019 (COVID-19) disease, caused by SARS-CoV-2 virus, occurred in Wuhan, Hubei Province, China, and rapidly spread worldwide [1,2]. COVID-19 is transmitted via droplets during the incubation period and throughout the course of illness [3]. Up to 20% of infected patients develop moderate-to-severe pneumonia and require hospitalization, and 5-10% are admitted to intensive care unit (ICU) for ventilation support [4–8]. According to recent studies, SARS-CoV-2 infection is not limited to the respiratory system and other organs can also be affected leading to a broad spectrum of signs. Recent studies have underscored the high frequency of acute kidney injury, proteinuria, and hematuria during COVID-19 [9,10]. Moreover, kidney involvement is burdened by a dramatic impact on patients' survival [9–11]. Here, we report a multicentric case series of patients with COVID-19 who developed acute kidney injury and/or proteinuria and underwent a kidney biopsy in the Paris and its metropolitan area.

RESULTS

Clinical characteristics and Radiologic findings

Forty-seven patients from nine Nephrology and ICU departments of Paris and its metropolitan area, including 38 (80.9%) men, were diagnosed with COVID-19 and underwent a kidney biopsy during the recent epidemic from March 8 through May 19, 2020. Of note, during the study period, more than 14000 patients with COVID-19 were admitted to the different hospitals of Assistance Publique-Hôpitaux de Paris, including more than 3000 (21.4%) patients referred to the ICU.

The diagnosis of COVID-19 was confirmed by SARS-CoV-2 RT-PCR nasal or pharyngeal swab specimens in 43 (91.5%) patients of cases. In four patients with negative RT-PCR, the diagnosis was established on the results of a chest CT-scan, showing ground glass opacities with or without consolidative abnormalities highly suggestive of COVID-19 infection. Median age was 63 years IQR [52-69]. Forty-four (93.6%) patients had coexisting medical conditions, 31 (65.9%) having two or more conditions (**Table 1**). Most frequent comorbidities included hypertension (66%), diabetes mellitus (27.7%), obesity (27.7%), and previous kidney disease (25.5%), including four patients with heart (n=1), lung (n=1) or kidney (n=2) transplantation. Of note, all patients were negative for human immunodeficiency virus (HIV), except one patient treated for such infection before the onset of COVID-19 and who had a stable and negative viral load during COVID-19 episode. The most common symptoms on admission included fever and chills (85.1%), cough (63.8%), shortness of breath (55.3%), and diarrhea (23.4%) (**Table 2**). All patients required hospital admission, including more than 50% of patients who required oxygen therapy on admission (WHO score ≥ 5, **Supplementary Table S4**). Of note, 20 (42.6%) patients did not require oxygen therapy initially (WHO score = [2-4]), but were hospitalized because of extra-respiratory features in the setting of COVID-19, including acute kidney injury and proteinuria. Chest CT-scan was performed in 43 patients (91.5%) within the 4 days IQR [1-9] after initial symptoms and revealed mild, moderate or severe lesions in 3 (7%), 19 (44.2%), and 21 (48.8%) patients, respectively (**Table 2**). During disease course, most patients developed severe inflammatory syndrome characterized by a median blood C-reactive protein level of 199 mg/L IQR [139-283], and severe hematological abnormalities, including anemia, lymphopenia, and thrombopenia in 38 (80.9%), 21 (45.7%), and 18 (39.1%) patients, respectively (**Supplementary Table S1**).

Renal laboratory findings

On admission, serum creatinine level was 158 µmol/L IQR [88-370], while the maximum value during disease course was 644 µmol/L IQR [385-768]. Overall, only one patient who presented with nephrotic syndrome had normal renal function, and 3 (6.4%), 2 (4.3%) and 41 (87.2%) patients experienced AKI stage I, II, and III, respectively. Thirty (63.8%) patients, including seven (23.3%) with preexisting chronic kidney disease required acute dialysis with a median delay of 14 days IQR [9-19] after initial symptoms. Seven out of 12 (58.3%) patients with preexisting chronic kidney disease required acute dialysis. All patients displayed a proteinuria > 0.3 g/g with a median urine protein-to-creatinine ratio (uPCR) of 2.52 g/g IQR [1.23-6.80]. Eighteen (40%) patients had a uPCR ≥ 3 g/g, while median serum albumin level was 21 g/L IQR [16-23]. Urine albumin-to-creatinine ratio was not measured in all patients at the time of kidney biopsy. Hematuria was observed in 22 (55%) patients. Other laboratory findings are detailed in **Supplementary Table S1**.

Kidney biopsy indications

Kidney biopsies, including two renal graft biopsies, were performed with a median delay of 18 days IQR [10-26] after initial symptoms. Seventeen patients were biopsied during their ICU stay because of stage III AKI or dialysis requirement, including two anuric patients. Thirteen patients underwent a kidney biopsy after ICU discharge because of persistent AKI and significant proteinuria. Finally, the remaining 17 kidney biopsies were performed in non-critically ill patients because of significant proteinuria (> 1 g/g) in all cases, associated with stage III AKI in all cases.

Overall, of the 47 patients, 19 (40.4%) displayed overt nephrotic syndrome with a mean proteinuria level of 12.1 g/g IQR 5.96-11.95] and a mean serum albumin level of 18.2 g/L IQR [16-22]. All 19 patients, except one, had concomitant AKI with a mean serum creatinine level

of 692 µmol/L IQR [370-880] at kidney biopsy. The remaining 28 patients with no nephrotic syndrome had AKI with a mean serum creatinine level of 569 µmol/L IQR [388-650] and a mean proteinuria level of 1.6 g/g IQR [0.97-2.32] (**Supplementary Table S2**).

Pathological analysis

Histopathological examination revealed two main patterns of kidney damage, i.e. tubulointerstitial injury and glomerular injury in 20 (42.6%) and 17 (36.2%), respectively (**Table 3**). Two patients (4.3%) displayed vascular lesions, including thrombotic microangiopathy and arteritis, consistent with a COVID-19-related vasculopathy. In the remaining 8 patients (17.0%), renal findings were consistent with alternative diagnosis (**Table 3**), which was most likely unrelated to COVID-19. Thirty-seven kidney biopsies were centrally reviewed by SF and detailed scoring of glomerular, tubular, interstitial and vascular lesions are provided in **Supplementary Table S3**.

Acute tubular injury was the dominant injury pattern in 20 (42.6%) cases. Various degrees of tubular damage were noticed, including loss of the brush border, flattening of the tubular epithelium, tubular microvacuolization, blebbing, and tubular cell and tubular basement membrane denudation (i.e acute tubular necrosis) **(Figure 1A and 1D)**. Interstitial infiltration by mononuclear cells was observed in 80% of cases (**Figure 1B**). Immunophenotyping was performed in four cases and showed the presence of CD3+ T lymphocytes and CD68+ macrophages. Associated lesions of diabetic nephropathy were observed in one case. Immunofluorescence study was negative for all cases of acute tubulointerstitial injury.

Focal segmental glomerulosclerosis (FSGS) represented the second dominant pattern in 17 patients, including collapsing (**Figures 2A-B**), not otherwise specified (**Figure 2C**), and tip lesion variants (**Figure 2D**) in 11, 5, and one cases, respectively. Collapsing glomerulopathy was associated with tubular microcystic changes in almost half of cases and PAS-positive protein

resorption droplets in proximal tubules in all cases (**Figure 1C**). Almost all patients harbored mild-to-severe acute tubular injury. Immunofluorescence study revealed segmental glomerular deposits of IgM and C3.

Predominant vascular lesions were also observed in two patients, including a case with thrombotic microangiopathy characterized by the presence of fibrin thrombi in a glomerulus, and a case with necrotizing arteritis. Both patients also harbored moderate lesions of acute tubular injury.

Finally, varying degrees of interstitial fibrosis and tubular atrophy, as well as chronic vascular lesions, were also present in a vast majority of patients regardless the main diagnosis. Ultrastructural examination by electron microscopy was performed in nine cases. No electron dense deposits were observed by electron microscopy in the patients without pre-existing kidney disease. No viral particles were observed. Interestingly, endothelial injury was noted including mild (62.5%) and moderate (32.5%) swelling of endothelial cells in the glomerular in eight cases, and peritubular capillaries in four cases. Tubuloreticular inclusions were observed in seven cases (**Figure 3**). Of note, diffuse effacement of podocytes foot processes was observed in seven cases, all of which corresponded to glomerular predominant lesions except one case with predominant tubular injury. Mild foot process effacement was also observed in a case with dominant tubular injury.

Anti-SARS-CoV-2 immunohistochemistry staining was performed on 16 kidney biopsies, including 7 patients with predominant acute tubular injury, 4 with collapsing glomerulopathy, 1 with focal segmental glomerulosclerosis and 4 with alternative diagnosis, and yielded negative results in all cases. Of note, appropriate controls were used, including SARS-CoV-2 positive placenta specimen and SARS-CoV-2 negative kidney biopsy tissues (**Figure 4**).

Clinicopathological correlations

During hospitalization, three profiles of severity could be distinguished based on the worst WHO progression scale. Five patients (10.6%) remained oxygen-free during the whole disease course (WHO score between 2 and 4). Eleven (23.4%) with a WHO score equal to 5 required up to 6 L/min of oxygen therapy, whereas 31 (66%) with a WHO score ≥ 6 required higher amounts (≥ 9/L) of oxygen therapy and were referred to the ICU in 93.5% of cases.

All biopsies performed in the ICU showed dominant and severe acute tubular injury. None had evidence for glomerular involvement by light microscopy analysis, except one with a preexisting chronic diabetic nephropathy. Most (72.7%) patients with dominant acute tubular injury had experienced severe hemodynamic instability compared to only 16% of patients with alternative pathological diagnosis ($p<0.001$). Nevertheless, six (27.3%) patients with isolated acute tubular injury and six (35.3%) patients who underwent the biopsy in the ICU did not experience prominent hemodynamic instability. We did not observe a significant association between the need for vasopressor and the severity of acute tubular injury across the different pathological patterns ($p=0.45$). Moreover, the range of urine protein-to-creatinine ratio was unexpectedly high (> 1 g/g) in 70% of patients with acute tubular injury. Nevertheless, the urine albumin level was not available for all patients but was not markedly increased arguing against glomerular proteinuria in these patients with acute tubular injury and significant proteinuria. Median albumin level was 19 g/L IQR [16-23], 18 g/L IQR[16-22], 22 g/L [20-22], and 21.5 g/L IQR [20-25.1] for patients with acute tubular injury, collapsing glomerulopathy, focal segmental glomerulosclerosis, and other alternative diagnosis respectively ($p = 0.75$). Overt nephrotic syndrome was observed in 6 (54.5%) and 5 (83.3%) patients with collapsing glomerulopathy and focal segmental glomerulosclerosis, respectively.

Kidney biopsies performed after ICU discharge or in non-critically ill patients displayed admixed type of renal lesions. Collapsing glomerulopathy, and FSGS, coincided with mild,

moderate and severe COVID-19 pneumonia in 4 (23.5%), 6 (35.3%), and 7 (41.2%) patients, respectively. Only 5 (29.4%) of the 17 patients with collapsing glomerulopathy and/or FSGS were admitted to the ICU. Notably, apolipoprotein 1 (*APOL1*) genotyping was available in 11 patients with either collapsing glomerulopathy (n=7) or FSGS (n=4). All the 7 patients with collapsing glomerulopathy were of African ancestry and harbored highly at-risk combinations of *APOL1* variants, including either *G1/G1* or *G1/G2*. By contrast, only two of the four patients with other FSGS variants displayed a *G1/G2* combination, whereas the remaining two had either *G0/G2* (not otherwise specified variant) or *G0/G0* (tip variant) genotypes.

In order to establish whether the profile of kidney lesions correlated with the severity of COVID-19, we compared the main kidney pathological findings in the 30 patients admitted to the ICU to the 17 remaining patients (**Table 4**). Interestingly, the predominant pathological patterns differed significantly between both groups with ICU patients displaying more frequently predominant acute tubular injury (66.7% versus 0%, $p < 0.001$). Such findings were also observed when comparing the sickest patients (with a worst WHO score ≥ 6) to those with the WHO score < 6.

Management and outcome

Antibiotherapy based on penicillin, 3G cephalosporin combined with macrolides was given in 40 patients (85.1%) during hospitalization (**Table 45**). Only a minority of patients received hydroxychloroquine or anti-IL6 antibodies. Seventeen patients (36.2%) were administered antiviral therapy, including a combination of lopinavir and ritonavir in 10 (58.8%) patients.

30 patients (63.8%) were transferred to the ICU with a median delay of 6 days IQR [3-11] after initial symptoms, including 28 (93.3%) who required mechanical ventilation. 26 patients (86.7%) developed acute respiratory distress syndrome, while 20 (66.7%) experienced severe hemodynamic instability, and 12 (40%) developed ventilator-associated pneumonia.

After a median follow-up of 37 days IQR [24-54], 16 patients (53.3%) were still on dialysis including 10 patients (62.5%) with acute tubular injury, 5 (31.3%) with FSGS, and one with myeloma cast nephropathy. Five patients of the 12 who had a preexisting chronic kidney disease remained dialysis dependent at last follow-up. Dialysis was discontinued in 14 patients (46.7%), including nine patients (64.3%) who developed acute tubular injury, 4 (28.6%) with FSGS, and 1 with PLA2R-positive membranous nephropathy. No clear correlation was observed between chronicity on the kidney biopsy and recovery and dialysis-dependence at last follow-up. Serum creatinine level in dialysis-free patients was 205 µmol/L IQR [125-261]. Nine patients (19.1%) died either from COVID-19 or related-adverse events (**Table 4**), but no autopsy was undertaken.

DISCUSSION

We report herein a multicentric case series describing the clinical and histopathological spectrum of kidney damage in patients with COVID-19. Two main histopathological patterns were identified: acute tubular (and interstitial) lesions, and glomerular injury mainly consisting of collapsing glomerulopathy. A minority of patients may display alternative diagnosis, which were likely unrelated to COVID-19, underscoring the value of the kidney biopsy in this setting.

Initial histopathological studies dealing with COVID-19 and kidney involvement have been limited to autopsies [12,13]. More recent series have addressed the renal lesions in patients with COVID-19, reporting cases of collapsing glomerulopathy and acute tubular injury [14–17]. In the present study, we addressed early renal events in patients with varying degrees of COVID-19 pneumonia, reporting both glomerular and tubular injury. Isolated or combined acute tubular injury represents the predominant pattern, seen mostly in patients with serious forms of COVID-19. Albeit hypoperfusion has been proposed as an underlying mechanism in

these patients, almost one-third of patients with acute tubular injury or those admitted to the ICU did not experience prominent hemodynamic instability. These findings suggest that additional factors may likely contribute to tubular damage in the setting of COVID-19 pneumonia, including tissue hypoxia, rhabdomyolysis, and the so-called “cytokine storm”, as suggested by the identification by electron microscopy of interferon footprints in glomerular capillaries endothelial cells. Hypercoagulability and microangiopathy with complement cascade activation are also to consider [18]. The swelling of endothelial cells, as assessed by electron microscopy, points to endothelial injury as a potential mechanism to explain severe renal damage, as also reported in other organs, such as lungs and heart [19–22]. Alternatively, a direct viral cytotoxicity on renal cells has been widely debated in the literature, mainly supported by the expression in the kidneys of proteins that facilitate SARS-CoV-2 infection, including Angiotensin Converting Enzyme 2, and Transmembrane protease serine 2 [18,23,24]. Recent reports have shown positive immunohistochemical staining for SARS-CoV-2 nucleocapsid protein in post-mortem kidneys [12,13,25]. Nevertheless, the presence of viral particles within tubular epithelial cells and podocytes remains controversial [14,26,27]. Similarly to recent reports, we did not observe kidney expression of SARS-CoV-2 nucleoprotein in our study, suggesting the absence of kidney infection by the virus [15,16,28].

In addition to tubular damage, COVID-19 may be associated with notable glomerular lesions, particularly in non-critically ill patients, widening the spectrum of COVID-19-associated nephropathy. In line with recent case reports, collapsing glomerulopathy represents the predominant histopathological pattern of glomerular lesions seen in the course of COVID-19 [14,29–33]. This peculiar variant of FSGS is characterized by segmental or global glomerular tuft collapse with hypertrophy and hyperplasia of the overlying podocytes [34,35]. Accompanying acute tubular injury, tubular dilations with microcyst formation and interstitial

inflammation, as commonly seen in HIV-associated nephropathy [36], were less prominent in patients with COVID-19. As in our series, all patients with COVID-19-associated collapsing glomerulopathy previously reported in the literature displayed AKI, heavy proteinuria, and hypoalbuminemia [29–33]. Noteworthy, collapsing glomerulopathy, and FSGS, coincided with varying degrees of severity COVID-19 pulmonary involvement, suggesting that, unlike to patients with dominant tubulointerstitial lesions, COVID-19-associated glomerular injury is likely multifactorial and somehow unrelated to the severity of respiratory involvement [37]. In this line, some cases of glomerular involvement may also occur after the recovery of respiratory signs [37]. Because collapsing glomerulopathy and FSGS may be primary or secondary to a wide range of causes, including viral infections and inflammatory diseases [35], many authors suggested a similar causality with SARS-CoV-2 [38,39]. Nevertheless, and as far as we know, several groups failed to detect SARS-CoV-2 RNA by *in situ* hybridization or RT-PCR on kidney biopsies [29–31,33,40]. The term of "COVID-19-associated nephropathy" should thus be preferred to that of "SARS-CoV-2 nephropathy" to stress the point that the demonstration of a direct or indirect role of SARS-CoV-2 in kidney injury remains an unsolved issue to date. Importantly, we and other have identified a crucial role of *APOL1* high risk variants (i.e. *G1/G1*, *G1/G2* or *G2/G2* genotypes) in the risk of COVID-19-associated collapsing glomerulopathy [14]. A plausible model is that COVID-19, irrespectively of a direct or indirect role of SARS-CoV-2, acts as a « second hit » that results in podocyte injury, and various histopathological patterns depending on the genetic background [14].

In conclusion, the spectrum of COVID-19-associated nephropathy includes both tubular and glomerular lesions with likely distinctive pathophysiological mechanisms. Kidney biopsy is very helpful to determine the precise nature of renal lesions during COVID-19 course

and guide subsequent management. Tubular damage is predominantly observed in most severe respiratory cases and may be related to hemodynamic changes and other additional factors. Glomerular lesions, including collapsing glomerulopathy and FSGS are predominantly observed in non-critically ill patients without an obvious correlation with the severity of respiratory signs. The carriage of *APOL1* high-risk variants is crucial to understand the pattern of glomerular lesions. While a direct or indirect effect of SARS-CoV-2 on kidney lesions is a current "hot topic" in the Nephrology field, further investigations using trustworthy tools are necessary to decipher the pathophysiology of COVID-19-associated kidney damage. Finally, and beyond diagnosis, it will also be interesting to correlate kidney biopsy findings to renal recovery and outcome at distance of COVID-19 episode.

CONCISE METHODS

Study population

We included all patients with COVID-19 who underwent a kidney biopsy in nine different Nephrology and ICU departments in the Paris region, from March 08 to May 19, 2020. A case of COVID-19 was defined by a positive result on a reverse-transcriptase polymerase chain reaction (RT-PCR) assay based on the World Health Organization (WHO) standard and targeting the *SARS-CoV-2 E* gene and *RdRp* gene of a specimen collected on a nasopharyngeal swab. In case of negative RT-PCR, a second RT-PCR could be performed. Alternatively, the diagnosis could also be established on the results of a chest CT-scan, showing ground glass opacities with or without consolidative abnormalities highly suggestive of COVID-19 infection. The study was approved by the local institutional review board as minimal risk research using retrospective data collected for routine clinical practice. A declaration on the Commission

Nationale de l'Informatique et des Libertés (CNIL) was made according to the French law (Loi Jardé and its subsequent amendments).

Data Collection

Patients' data were obtained through the retrospective review of the medical electronic records. Three patients have already been reported as single cases [32,33]. Demographic data and comorbidities included age, sex, hypertension, diabetes mellitus, body mass index, and other coexisting comorbidities, including chronic kidney disease, cardiovascular disease, use of angiotensin receptor blockers or angiotensin-converting enzyme inhibitors, and other notable past medical history. Date and nature of presenting signs, and oxygen saturation and oxygen level to reach an oxygen saturation ≥ 94% were collected. The WHO progression scale (**Supplementary Table S4**) was used to establish three groups of severity on admission and during follow-up including: (1) ambulatory or hospitalized patients who did not require oxygen therapy (WHO score = [2-4]); (2) hospitalized patients who needed oxygen therapy up to 6 L/min by mask or nasal prongs (WHO score = 5); and (3) hospitalized patients who required higher amounts of oxygen therapy by non-invasive ventilation or intubation and mechanical ventilation (WHO score ≥ 6). The maximum level of oxygen before ICU transfer, use of non-invasive and mechanical ventilation, severe events during hospitalization, including acute respiratory distress syndrome, thrombosis, bleeding, cardiac arrythmia, sepsis and death were also recorded. Dates of admission, transfer to the ICU, initiation of dialysis, mechanical ventilation, discharge from ICU and from hospital were collected. All laboratory tests and radiologic assessments were performed at the discretion of the physician. Laboratory data included the result of the SARS-CoV-2 RT-PCR nasal or pharyngeal swab specimens, and the values of biological parameters on admission and during hospitalization (extreme values): serum levels of electrolytes, albumin, lactate dehydrogenases, ferritin, C-reactive protein,

procalcitonin, D-Dimers, fibrinogen, and hemoglobin, and lymphocyte, neutrophil, and platelet counts. Renal parameters included serum creatinine, urine protein and urine red and white blood cells count. Acute kidney injury (AKI) was scored according to the 2012 Kidney Disease: Improving Global Outcomes Clinical Practice Guideline for AKI (https://kdigo.org/guidelines/acute-kidney-injury/). Proteinuria and nephrotic range proteinuria were defined by urine protein > 0,3 g/day and ≥ 3 g/day, respectively. The results of chest CT-scan were graded as mild, moderate and severe according to the extent of pulmonary lesions as follows: <10%, 10-25%, and 25-50% of the lung parenchyma. The administration of antibiotics and other notable drugs, such as anti-IL6 antibodies, hydroxychloroquine was also recorded. Patient data were censored at the time of data cutoff, which occurred on May 30, 2020.

Kidney biopsy processing

Kidney biopsies specimens were immersed immediately after removal in Alcohol-Formalin-Acetic acid (AFA), embedded in paraffin, cut into 3 µm sections and stained with hematoxylin-eosin-saffron, periodic acid-Schiff, Masson's Trichrome and Jones or Marinozzi methenamine silver. Immunofluorescence study was performed in all cases. The presence of immune deposits was determined based on the immunostaining for IgG, IgM, IgA, C3, C1q, kappa, and lambda light chains. Electron microscopy analysis was performed in nine cases according to the following protocol: samples were fixed in 2.5% glutaraldehyde in 0.1 mmol/L cacodylate buffer (pH 7.4) at 4°C. Fragments were then post-fixed in 1% osmium tetroxide, dehydrated using alcohol series, and embedded in epoxy resin. Semithin sections (0.5 µm) were stained using toluidine blue. Ultrastructure sections (80 nm) were contrast-enhanced using uranyl acetate and lead citrate, and they were examined using a JEOL 1010 electron microscope (JEOL, Ltd., Tokyo, Japan).

All kidney biopsies were analyzed locally by experts in the renal pathology (SF, CM, DB, IB, AS, AM) from 5 French Departments belonging to the Club Francophone de Pathologie Rénale (CFPR) group. 37 renal biopsy specimens were centrally reviewed by SF to establish a scoring of renal lesions by light microscopy. The following lesions: interstitial fibrosis, edema, inflammatory infiltrate and acute tubular injury were estimated semi-quantitatively and classified as mild if they affected up to 25% of the cortical area, moderate between 26 and 50%, and severe beyond 50%. Vascular lesions were evaluated according the severity of the thickness of the intima for arteries and proportion of vessels showing hyalinosis for arterioles. Immunohistochemistry staining was performed on 16 renal tissue sections from our series (7 patients with predominant acute tubular necrosis, 4 with collapsing glomerulopathy, 1 with focal segmental glomerulosclerosis and 4 with alternative diagnosis) on a semi-automated Bond-III Leica instrument using anti-SARS-CoV-2 primary antibody (Abclonal, rabbit pAB, 2019-nCoV N Protein, citrate pH6 heat pretreatment, 1:200). The sections were treated with a solution of peroxidase-labeled streptavidin and the color reaction was developed by incubation with 3,3'-diaminobenzidine (DAB) according to the Bond Polymer Refine detection kit instructions. The nuclei were then counterstained with hematoxylin. Positive controls (SARS-CoV-2 positive placental and broncho-alveolar specimens) and negative (SARS-CoV-2 negative renal biopsy and placenta) controls were done and yielded appropriate results.

Statistical analysis

Descriptive statistics were used to summarize the data. Results are reported as medians with interquartile range [IQR] for continuous variables and counts and percentages for categorical variables. Univariate analyses were performed using the Kruskal-Wallis test, and the $\chi 2$ or Fisher exact test, as appropriate. A $p\text{-value} < 0.05$ was considered as significant.

CONFLICT OF INTEREST STATEMENT

The authors have no conflicts of interest to declare

FIGURE LEGENDS

Figure 1. Tubulointerstitial and vascular lesions. A, Acute tubular injury. Dilatation and flattening of the tubular epithelium with some proteinaceous casts (Trichrome stain, x100). **B**, Mild interstitial edema and mononuclear inflammation, associated with acute tubular injury, and ischemic glomerulus (Trichrome stain, x200). **C**, Various tubular changes observed in case of collapsing glomerulopathy with dilatation of tubules filled with hyaline casts (*star*), and cytoplasmic protein droplets (arrow) (Trichrome stain, x61). **D**, Marked acute tubular injury with cell fragments within the tubular lumen and flattening of the tubular epithelium (Trichrome stain, x400). Scale bars: 50 µm.

Figure 2. Glomerular lesions in the course of COVID-19. A, Light microscopy examination showing a case of collapsing glomerulopathy characterized by global collapse of glomerular capillaries associated with marked hyperplasia of podocytes, many of which display abundant cytoplasmic protein droplets (Trichrome stain, x200). **B**, The same glomerulus with the Marinozzi methenamine silver stain highlighting the global collapse of capillaries associated with hyperplasia and swelling of overlying podocytes (Marinozzi methenamine silver stain, x200). **C**, Not otherwise specified variant of focal segmental glomerulosclerosis showing hyalinosis in this advanced sclerotic lesion. There are also adhesions of the sclerotic segments to Bowman's capsule (Trichrome stain, x400). **D**, Tip lesion variant of focal segmental glomerulosclerosis and overlying podocytes at the origin of the proximal tubule (Trichrome stain, x200). Scale bars: 50 µm.

Figure 3. Ultrastructural examination by electron microscopy. Electron microscopy (magnification x 10000) showing numerous tubuloreticular inclusions (arrows) within glomerular endothelial cell and partial foot processes effacement (black asterisks). P: podocyte, L: capillary lumen, white asterisk: GBM. Scale bar: 1 µm.

Figure 4. Anti-SARS-CoV-2 immunohistochemistry staining. Illustration of anti-SARS-CoV-2 negative staining in patients with COVID-19 and collapsing glomerulopathy (**A and B**), and predominant acute tubular injury (**C and D**). Background peroxidase activity is illustrated by anti-SARS-CoV-2 immunostaining in kidney tissue specimen from COVID-19 negative patients (**E and F**), including a patient with HIV-associated nephropathy. The specificity of anti-SARS-CoV-2 antibody is demonstrated by the staining of placenta specimen from patients with or without COVID-19 (**G and H**). Scale bars: 50 µm.

Table 1. Demographic data and coexisting comorbidities

	Patients (n=47)
Demographic data	
- Age (years)	63 [52-69]
- Male gender	38 (80.9%)
- Weight (kg)	85.5 [73-96.2]
- BMI (kg/m²)	26.6 [24.6-30.0]
Coexisting conditions	
- ≥ 2 comorbidities	31 (66,0%)
- Blood hypertension	31 (66.0%)
- ACEi use	11 (23.4%)
- ARB use	10 (21.3%)
- Dyslipidemia	14 (29.8%)
- Obesity (BMI > 30 kg/m²)	13 (27.7%)
- Diabetes mellitus	13 (27.7%)
- Smoking	10 (21.3%)
- Chronic kidney disease	12 (25.5%)
- Stage IIIa	5 (41.7%)
- Stage IIIb	5 (41.7%)
- Stage IV	2 (16.7%)
- Chronic cardiac disease	10 (21.3%)
- Chronic respiratory disease	1 (2.1%)
- Cancer	8 (17.0%)
- Immunosuppressive drugs	8 (17.0%)

Abbreviations: BMI: body mass index; ACEi: angiotensin converting enzyme inhibitors; ARB: angiotensin II receptor blockers.

Table 2. Diagnostic features

	Patients (n=47)
Presenting clinical symptoms	
- Fever	40 (85.1%)
- Cough	30 (63.8%)
- Shortness of breath	26 (55.3%)
- SpO2 (%)	91 [89-97]
- Oxygen therapy (L/min)	1 [0-5]
- initial WHO score [2-4]	21 (44.7%)
- initial WHO score [5]	16 (34.0%)
- initial WHO score ≥6	10 (21.3%)
- Diarrhea	11 (23.4%)
SARS-CoV2 RT-PCR	
- Positive RT-PCR nasal or pharyngeal swab specimens	43 (91.5%)
- Time from initial symptoms (days)	3 [1-7]
Chest CT-Scan	
- CT Scan performed	43 (91.5%)
- Time from initial symptoms (days)	4 [1-9]
- Mild	3 (7%)
- Moderate	19 (44.2%)
- Severe	21 (48.8%)

Abbreviations: SpO2: oxygen saturation; RT-PCR: reverse transcriptase-polymerase chain reaction; CT: computed tomography.

Table 3. Renal findings on admission and at the time of kidney biopsy

	Patients (n=47)
Baseline serum creatinine level (µmol/L)	87 [75-118]
Renal parameters on admission	
- Serum creatinine level (µmol/L)	158 [88-370]
- Serum Albumin level (g/L)	25 [22-31]
- uPCR (g/g)	1.86 [0.82-7.79]
- Hematuria	22 (55.0%)
- Leukocyturia	27 (67.5%)
Renal status at the time of kidney biopsy	
- Time from initial symptoms (days)	18 [10-26]
- uPCR (g/g)	2.52 [1.23-6.80]
- uPCR ≥ 3 g/g	18 (40.0%)
- Albuminemia (g/dL)	21 [16-23]
- Albuminemia < 30 g/L	40 (95.2%)
- Serum creatinine level (µmol/L)	644 [385-768]
- Acute kidney injury	
- No	1 (2.1%)
- KDIGO 1	3 (6.4%)
- KDIGO 2	2 (4.3%)
- KDIGO 3	41 (87.2%)
Main histopathological findings	
- Predominant acute tubular necrosis	20 (42.6%)
- Focal segmental glomerulosclerosis	17 (36.2%)
- Collapsing glomerulopathy	11 (64.7%)
- Not otherwise specified	5 (29.4%)
- Tip lesion	1 (5.9%)
- Vascular nephropathy	2 (4.3%)
- Thrombotic microangiopathy	1
- Arteritis	1
- Other diagnoses[#]	8 (17%)
- AA amyloidosis	1
- PLA2R (+) membranous nephropathy	2
- Extracapillary glomerulonephritis	1
- IgA nephropathy	1
- Myeloma cast nephropathy	1
- Calcineurin inhibitors-related toxicity	1
- IF/TA grade 3*	1

Abbreviations: uPCR: Urine Protein-to-Creatinine ratio; IF/TA: Interstitial Fibrosis and Tubular Atrophy. * On kidney graft biopsy. [#] Please note that no case of anti-GBM disease was observed.

Table 4. Comparison of the main histopathological pattern of kindey lesions in respect to the severity of COVID-19 (as assessed by ICU admission)

	ICU patients (n=30)	**non-ICU patients** (n=17)	***p***
Predominant ATN	20 (66.7%)	0 (0%)	*<0.001*
CG/FSGS	3+2 (16.7%)	8+4 (70.6%)	*<0.001*
Vascular Nx	2 (6.7%)	0 (0%)	*ns*
Other	3 (10%)	5 (29.4%)	*ns*

Abbreviations: ATN: acute tubular necrosis; CG: collapsing glomerulopathy; FSGS: focal and segmental glomerulosclerosis; Nx: nephropathy

Table 5. Initial management and outcome

	Patients (n=47)
Treatment	
- Antibiotherapy	40 (85.1%)
- Azithromycin	22 (46.8%)
- Hydroxychloroquine	9 (19.1%)
- Anti-IL6 antibodies	2 (4.3%)
- Antiviral treatment	17 (36.2%)
Respiratory evolution	
- worst WHO score [2-4]	5 (10.6%)
- worst WHO score [5]	11 (23.4%)
- worst WHO score ≥6	31 (66.0%)
Acute dialysis	30 (63.8%)
Transfer to the intensive care unit	30 (63.8%)
- Time from initial symptoms (days)	6 [3-11]
- Mechanical ventilation	28 (93.3%)
- ECMO	3 (10%)
- Vasopressive support	20 (66.7%)
- Acute respiratory syndrome	26 (86.7%)
- Ventilator-associated pneumonia	12 (40%)
Outcome	
- Renal status at last follow-up	
- Follow-up (days)	37 [24-54]
- Ongoing dialysis	16 (34.0%)
- Serum creatinine level (µmol/L)*	205 [125-261]
- Other complications	
- Atrial fibrillation	6 (12.8%)
- Bleeding	6 (12.8%)
- Pulmonary embolism	2 (4.3%)
- Other thrombosis	5 (10.6%)
- Death	9 (19.1%)
- Delay from initial symptoms (days)	19 [16-25]
- Refractory shock	4 (44.4%)
- Refractory Acute respiratory syndrome	5 (55.6%)
- Status at last follow up of the surviving patients	38 (80.9%)
- Discharge from hospital	26 (68.4%)
- Discharge from ICU but still on hospital	12 (31.6%)

Abbreviations: IL6: Interleukin 6; MV: Mechanical ventilation: ECMO: Extracorporeal Membrane Oxygenation; ARDS: Acute respiratory distress syndrome; RRT: Renal replacement therapy. * After exclusion of patients who required renal replacement therapy at last follow-up.

SUPPLEMENTARY MATERIAL

Supplementary Table S1. Initial and extreme laboratory findings during disease course.

Supplementary Table S2. Kidney biopsy indications in the 47 patients with COVID-19.

Supplementary Table S3. Detailed renal lesions scoring of 37 kidney biopsies.

Supplementary Table S4. WHO progression scale.

REFERENCES

1. Huang C, Wang Y, Li X, Ren L, Zhao J, Hu Y, Zhang L, Fan G, Xu J, Gu X, Cheng Z, Yu T, Xia J, Wei Y, Wu W, Xie X, Yin W, Li H, Liu M, Xiao Y, Gao H, Guo L, Xie J, Wang G, Jiang R, Gao Z, Jin Q, Wang J, Cao B. Clinical features of patients infected with 2019 novel coronavirus in Wuhan, China. Lancet Lond Engl 2020; 395:497–506.
2. Chen T, Wu D, Chen H, Yan W, Yang D, Chen G, Ma K, Xu D, Yu H, Wang H, Wang T, Guo W, Chen J, Ding C, Zhang X, Huang J, Han M, Li S, Luo X, Zhao J, Ning Q. Clinical characteristics of 113 deceased patients with coronavirus disease 2019: retrospective study. BMJ 2020; 368:m1091.
3. Lauer SA, Grantz KH, Bi Q, Jones FK, Zheng Q, Meredith HR, Azman AS, Reich NG, Lessler J. The Incubation Period of Coronavirus Disease 2019 (COVID-19) From Publicly Reported Confirmed Cases: Estimation and Application. Ann Intern Med 2020; .
4. Yang X, Yu Y, Xu J, Shu H, Xia J, Liu H, Wu Y, Zhang L, Yu Z, Fang M, Yu T, Wang Y, Pan S, Zou X, Yuan S, Shang Y. Clinical course and outcomes of critically ill patients with SARS-CoV-2 pneumonia in Wuhan, China: a single-centered, retrospective, observational study. Lancet Respir Med 2020; .
5. Wang D, Hu B, Hu C, Zhu F, Liu X, Zhang J, Wang B, Xiang H, Cheng Z, Xiong Y, Zhao Y, Li Y, Wang X, Peng Z. Clinical Characteristics of 138 Hospitalized Patients With 2019 Novel Coronavirus-Infected Pneumonia in Wuhan, China. JAMA 2020; .
6. Young BE, Ong SWX, Kalimuddin S, Low JG, Tan SY, Loh J, Ng O-T, Marimuthu K, Ang LW, Mak TM, Lau SK, Anderson DE, Chan KS, Tan TY, Ng TY, Cui L, Said Z, Kurupatham L, Chen MI-C, Chan M, Vasoo S, Wang L-F, Tan BH, Lin RTP, Lee VJM, Leo Y-S, Lye DC, Singapore 2019 Novel Coronavirus Outbreak Research Team. Epidemiologic Features and Clinical Course of Patients Infected With SARS-CoV-2 in Singapore. JAMA 2020; .

7. Wu Z, McGoogan JM. Characteristics of and Important Lessons From the Coronavirus Disease 2019 (COVID-19) Outbreak in China: Summary of a Report of 72 314 Cases From the Chinese Center for Disease Control and Prevention. JAMA 2020; .
8. Livingston E, Bucher K. Coronavirus Disease 2019 (COVID-19) in Italy. JAMA 2020; .
9. Pei G, Zhang Z, Peng J, Liu L, Zhang C, Yu C, Ma Z, Huang Y, Liu W, Yao Y, Zeng R, Xu G. Renal Involvement and Early Prognosis in Patients with COVID-19 Pneumonia. J Am Soc Nephrol JASN 2020; .
10. Hirsch JS, Ng JH, Ross DW, Sharma P, Shah HH, Barnett RL, Hazzan AD, Fishbane S, Jhaveri KD, Northwell COVID-19 Research Consortium, Northwell Nephrology COVID-19 Research Consortium. Acute kidney injury in patients hospitalized with COVID-19. Kidney Int 2020; .
11. Cheng Y, Luo R, Wang K, Zhang M, Wang Z, Dong L, Li J, Yao Y, Ge S, Xu G. Kidney disease is associated with in-hospital death of patients with COVID-19. Kidney Int 2020; 97:829–838.
12. Diao B, Wang C, Wang R, Feng Z, Tan Y, Wang H, Wang C, Liu L, Liu Y, Liu Y, Wang G, Yuan Z, Ren L, Wu Y, Chen Y. Human Kidney is a Target for Novel Severe Acute Respiratory Syndrome Coronavirus 2 (SARS-CoV-2) Infection. MedRxiv 2020; 2020.03.04.20031120.
13. Su H, Yang M, Wan C, Yi L-X, Tang F, Zhu H-Y, Yi F, Yang H-C, Fogo AB, Nie X, Zhang C. Renal histopathological analysis of 26 postmortem findings of patients with COVID-19 in China. Kidney Int 2020; .
14. Wu H, Larsen CP, Hernandez-Arroyo CF, Mohamed MMB, Caza T, Sharshir M, Chughtai A, Xie L, Gimenez JM, Sandow TA, Lusco MA, Yang H, Acheampong E, Rosales IA, Colvin RB, Fogo AB, Velez JCQ. AKI and Collapsing Glomerulopathy Associated with COVID-19 and APOL1 High-Risk Genotype. J Am Soc Nephrol JASN 2020; .

15. Kudose S, Batal I, Santoriello D, Xu K, Barasch J, Peleg Y, Canetta P, Ratner LE, Marasa M, Gharavi AG, Stokes MB, Markowitz GS, D'Agati VD. Kidney Biopsy Findings in Patients with COVID-19. J Am Soc Nephrol JASN 2020; 31:1959–1968.
16. Sharma P, Uppal NN, Wanchoo R, Shah HH, Yang Y, Parikh R, Khanin Y, Madireddy V, Larsen CP, Jhaveri KD, Bijol V, Northwell Nephrology COVID-19 Research Consortium. COVID-19-Associated Kidney Injury: A Case Series of Kidney Biopsy Findings. J Am Soc Nephrol JASN 2020; 31:1948–1958.
17. Akilesh S, Nast CC, Yamashita M, Henriksen K, Charu V, Troxell ML, Kambham N, Bracamonte E, Houghton D, Ahmed NI, Chong CC, Thajudeen B, Rehman S, Khoury F, Zuckerman JE, Gitomer J, Raguram PC, Mujeeb S, Schwarze U, Shannon MB, De Castro I, Alpers CE, Najafian B, Nicosia RF, Andeen NK, Smith KD. Multicenter Clinicopathologic Correlation of Kidney Biopsies Performed in COVID-19 Patients Presenting With Acute Kidney Injury or Proteinuria. Am J Kidney Dis Off J Natl Kidney Found 2020; .
18. Batlle D, Soler MJ, Sparks MA, Hiremath S, South AM, Welling PA, Swaminathan S, COVID-19 and ACE2 in Cardiovascular, Lung, and Kidney Working Group. Acute Kidney Injury in COVID-19: Emerging Evidence of a Distinct Pathophysiology. J Am Soc Nephrol JASN 2020; .
19. Varga Z, Flammer AJ, Steiger P, Haberecker M, Andermatt R, Zinkernagel AS, Mehra MR, Schuepbach RA, Ruschitzka F, Moch H. Endothelial cell infection and endotheliitis in COVID-19. Lancet Lond Engl 2020; 395:1417–1418.
20. Teuwen L-A, Geldhof V, Pasut A, Carmeliet P. COVID-19: the vasculature unleashed. Nat Rev Immunol 2020; .
21. Escher R, Breakey N, Lämmle B. Severe COVID-19 infection associated with endothelial activation. Thromb Res 2020; 190:62.

22. Clerkin KJ, Fried JA, Raikhelkar J, Sayer G, Griffin JM, Masoumi A, Jain SS, Burkhoff D, Kumaraiah D, Rabbani L, Schwartz A, Uriel N. COVID-19 and Cardiovascular Disease. Circulation 2020; 141:1648–1655.
23. Sungnak W, Huang N, Bécavin C, Berg M, Queen R, Litvinukova M, Talavera-López C, Maatz H, Reichart D, Sampaziotis F, Worlock KB, Yoshida M, Barnes JL, HCA Lung Biological Network. SARS-CoV-2 entry factors are highly expressed in nasal epithelial cells together with innate immune genes. Nat Med 2020; 26:681–687.
24. Puelles VG, Lütgehetmann M, Lindenmeyer MT, Sperhake JP, Wong MN, Allweiss L, Chilla S, Heinemann A, Wanner N, Liu S, Braun F, Lu S, Pfefferle S, Schröder AS, Edler C, Gross O, Glatzel M, Wichmann D, Wiech T, Kluge S, Pueschel K, Aepfelbacher M, Huber TB. Multiorgan and Renal Tropism of SARS-CoV-2. N Engl J Med 2020; .
25. Farkash EA, Wilson AM, Jentzen JM. Ultrastructural Evidence for Direct Renal Infection with SARS-CoV-2. J Am Soc Nephrol JASN 2020; .
26. Miller SE, Brealey JK. Visualization of putative coronavirus in kidney. Kidney Int 2020; 0:
27. Calomeni E, Satoskar A, Ayoub I, Brodsky S, Rovin BH, Nadasdy T. Multivesicular bodies mimicking SARS-CoV-2 in patients without COVID-19. Kidney Int 2020; 0:
28. Best Rocha A, Stroberg E, Barton LM, Duval EJ, Mukhopadhyay S, Yarid N, Caza T, Wilson JD, Kenan DJ, Kuperman M, Sharma SG, Larsen CP. Detection of SARS-CoV-2 in formalin-fixed paraffin-embedded tissue sections using commercially available reagents. Lab Investig J Tech Methods Pathol 2020; 100:1485–1489.
29. Larsen CP, Bourne TD, Wilson JD, Saqqa O, Sharshir MA. Collapsing Glomerulopathy in a Patient With Coronavirus Disease 2019 (COVID-19). Kidney Int Rep 2020; .
30. Kissling S, Rotman S, Gerber C, Halfon M, Lamoth F, Comte D, Lhopitallier L, Sadallah S, Fakhouri F. Collapsing glomerulopathy in a COVID-19 patient. Kidney Int 2020; 0:

31. Peleg Y, Kudose S, D'Agati V, Siddall E, Ahmad S, Kisselev S, Gharavi A, Canetta P. Acute Kidney Injury Due to Collapsing Glomerulopathy Following COVID-19 Infection. Kidney Int Rep 2020; .
32. Gaillard F, Ismael S, Sannier A, Tarhini H, Volpe T, Greze C, Verpont MC, Zouhry I, Rioux C, Lescure F-X, Buob D, Daugas E. Tubuloreticular inclusions in COVID-19–related collapsing glomerulopathy. Kidney Int 2020; 0:
33. Couturier A, Ferlicot S, Chevalier K, Guillet M, Essig M, Jauréguiberry S, Collarino R, Dargelos M, Michaut A, Geri G, Roque-Afonso A-M, Zaidan M, Massy ZA. Indirect effects of severe acute respiratory syndrome coronavirus 2 on the kidney in coronavirus disease patients. Clin Kidney J no date; .
34. D'Agati VD, Fogo AB, Bruijn JA, Jennette JC. Pathologic classification of focal segmental glomerulosclerosis: a working proposal. Am J Kidney Dis Off J Natl Kidney Found 2004; 43:368–382.
35. D'Agati VD, Kaskel FJ, Falk RJ. Focal segmental glomerulosclerosis. N Engl J Med 2011; 365:2398–2411.
36. Rao TK, Filippone EJ, Nicastri AD, Landesman SH, Frank E, Chen CK, Friedman EA. Associated focal and segmental glomerulosclerosis in the acquired immunodeficiency syndrome. N Engl J Med 1984; 310:669–673.
37. Nasr SH, Kopp JB. COVID-19-Associated Collapsing Glomerulopathy: An Emerging Entity. Kidney Int Rep 2020; .
38. Bruggeman LA, Ross MD, Tanji N, Cara A, Dikman S, Gordon RE, Burns GC, D'Agati VD, Winston JA, Klotman ME, Klotman PE. Renal epithelium is a previously unrecognized site of HIV-1 infection. J Am Soc Nephrol JASN 2000; 11:2079–2087.

39. Chen P, Chen BK, Mosoian A, Hays T, Ross MJ, Klotman PE, Klotman ME. Virological synapses allow HIV-1 uptake and gene expression in renal tubular epithelial cells. J Am Soc Nephrol JASN 2011; 22:496–507.
40. Rossi GM, Delsante M, Pilato FP, Gnetti L, Gabrielli L, Rossini G, Re MC, Cenacchi G, Affanni P, Colucci ME, Picetti E, Rossi S, Parenti E, Maccari C, Greco P, Mario FD, Maggiore U, Regolisti G, Fiaccadori E. Kidney biopsy findings in a critically ill COVID-19 patient with dialysis-dependent acute kidney injury: a case against “SARS-CoV-2 nephropathy.” Kidney Int Rep 2020; 0:

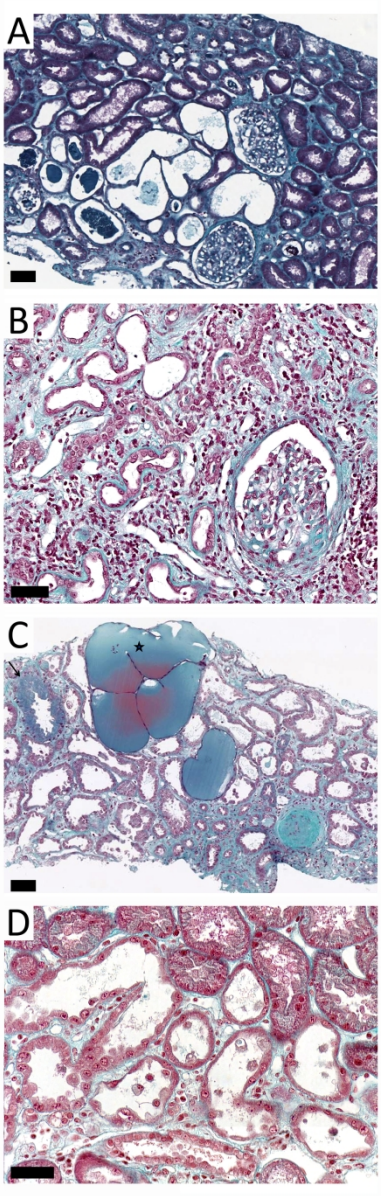

Figure 1. Tubulointerstitial and vascular lesions. A, Acute tubular injury. Dilatation and flattening of the tubular epithelium with some proteinaceous casts (Trichrome stain, x100). B, Mild interstitial edema and mononuclear inflammation, associated with acute tubular injury, and ischemic glomerulus (Trichrome stain, x200). C, Various tubular changes observed in case of collapsing glomerulopathy with dilatation of tubules filled with hyaline casts (star), and cytoplasmic protein droplets (arrow) (Trichrome stain, x61). D, Marked acute tubular injury with cell fragments within the tubular lumen and flattening of the tubular epithelium (Trichrome stain, x400). Scale bars: 50 μm.

101x307mm (300 x 300 DPI)

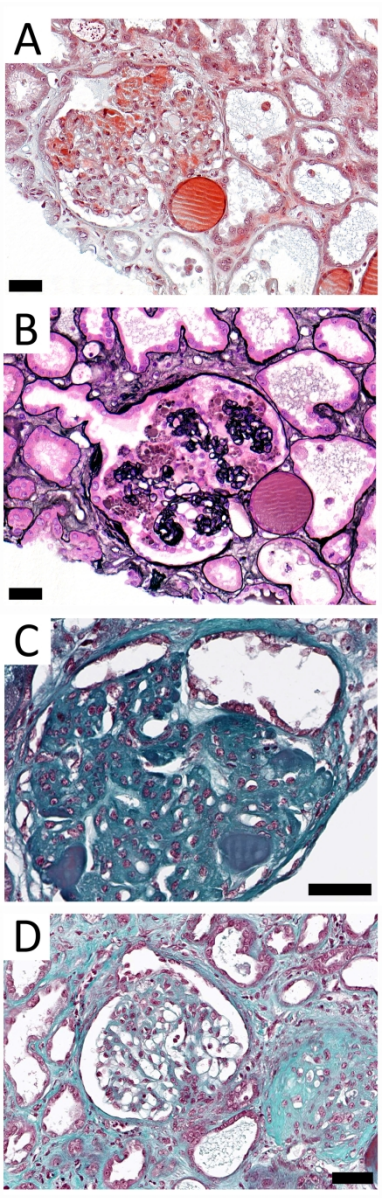

Figure 2. Glomerular lesions in the course of COVID-19. A, Light microscopy examination showing a case of collapsing glomerulopathy characterized by global collapse of glomerular capillaries associated with marked hyperplasia of podocytes, many of which display abundant cytoplasmic protein droplets (Trichrome stain, x200). B, The same glomerulus with the Marinozzi methenamine silver stain highlighting the global collapse of capillaries associated with hyperplasia and swelling of overlying podocytes (Marinozzi methenamine silver stain, x200). C, Not otherwise specified variant of focal segmental glomerulosclerosis showing hyalinosis in this advanced sclerotic lesion. There are also adhesions of the sclerotic segments to Bowman's capsule (Trichrome stain, x400). D, Tip lesion variant of focal segmental glomerulosclerosis and overlying podocytes at the origin of the proximal tubule (Trichrome stain, x200). Scale bars: 50 μm.

101x307mm (300 x 300 DPI)

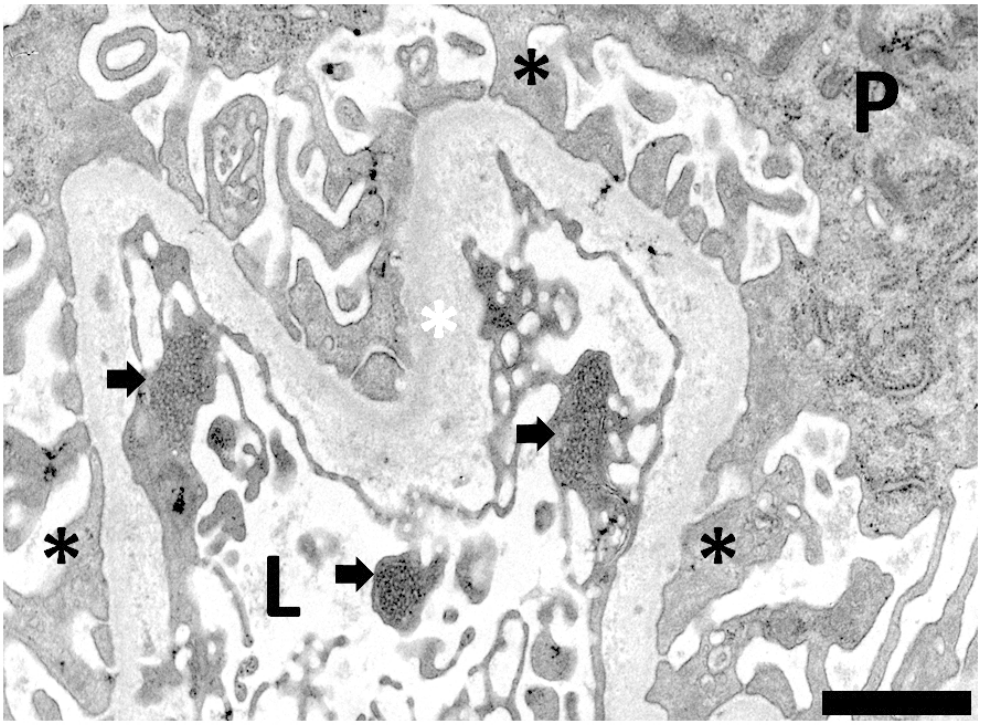

Figure 3. Ultrastructural examination by electron microscopy. Electron microscopy (magnification x 10000) showing numerous tubuloreticular inclusions (arrows) within glomerular endothelial cell and partial foot processes effacement (black asterisks). P: podocyte, L: capillary lumen, white asterisk: GBM. Scale bar: 1 µm.

76x56mm (300 x 300 DPI)

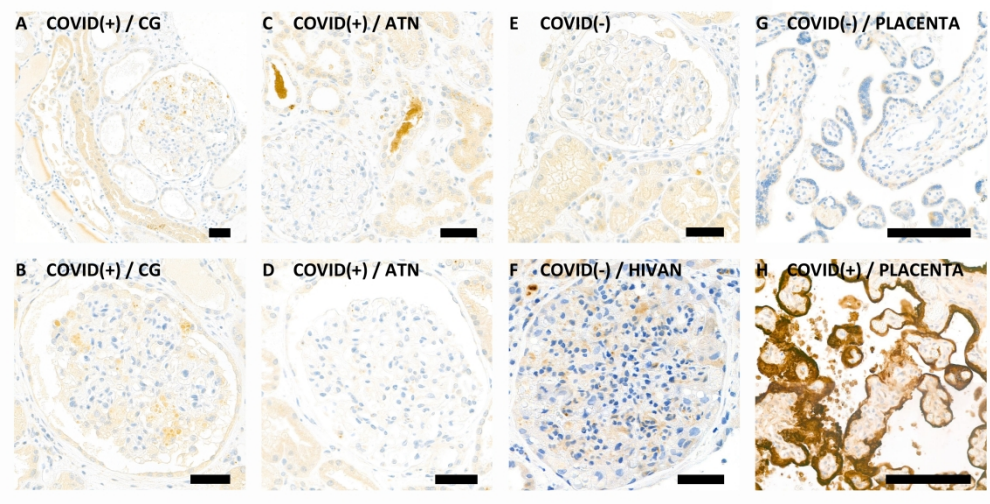

Figure 4. Anti-SARS-CoV-2 immunohistochemistry staining. Illustration of anti-SARS-CoV-2 negative staining in patients with COVID-19 and collapsing glomerulopathy (A and B), and predominant acute tubular injury (C and D). Background peroxidase activity is illustrated by anti-SARS-CoV-2 immunostaining in kidney tissue specimen from COVID-19 negative patients (E and F), including a patient with HIV-associated nephropathy. The specificity of anti-SARS-CoV-2 antibody is demonstrated by the staining of placenta specimen from patients with or without COVID-19 (G and H). Scale bars: 50 μm.

324x164mm (300 x 300 DPI)